Electronic Supplementary Material (ESI) for Environmental Science: Atmospheres.

Supplementary Information for:

Environmentally persistent free radicals in indoor particulate matter, dust, and on surfaces

A. Filippi[1], R. Sheu[2,3], T. Berkemeier[1], U. Pöschl[1], H. Tong*[1,4], D.R. Gentner*[1, 2, 5]

[1] Multiphase Chemistry Department, Max Planck Institute for Chemistry, 55128 Mainz, Germany

[2] Department of Chemical and Environmental Engineering, Yale University, New Haven, CT 06511, USA

[3] Department of Environmental Health and Engineering, Johns Hopkins University, Baltimore, MD 21218, USA

[4] Department of Civil and Environmental Engineering, The Hong Kong Polytechnic University, Kowloon, Hong Kong, China

[5] Solutions for Energy, Air, Climate and Health (SEARCH), School of the Environment, Yale University, New Haven, CT 06511, USA

Additional Methods Information

The indoor site was a multi-floor apartment with entry on the ground floor of a multi-unit building in central Mainz, Germany with a predominantly-open floorplan and modern renovations, but no forced-air handling (i.e. HVAC) system for heating/cooling. The 2 residents were non-smokers and cooking appliances (stove, oven, toaster) were electrically powered. The researchers note that there was active mold growth in part of the apartment at the very end of the campaign (Table S1) due to a water intrusion issue, yet the final PM sample was comparable to outdoor EPFR concentrations at that time (Figure 1a). The outdoor site for PM sampling in this study has been used in prior work[1] and is thus utilized in this study as a well-characterized outdoor reference site.

The samplers for collection of particulate matter consisted of a vacuum pump, a mass flow controller (Mass Stream < 70 L min^{-1}, M+W instruments), and a 47 mm single stage PFA filter assembly (Savillex Corp.) with a 47 mm PTFE membrane disc filter with support ring (46 µm thick, Pall Corporation), all connected by ¼ inch Teflon tubing. At the indoor location (located in the kitchen), the sampling rate controlled by the mass flow controller was set to 16 L min^{-1}, while the sampler outside was operated at 17 L min^{-1}. At the completion of the PM sampling campaign, samples were collected to examine the accumulated EPFR on surfaces and in dust. Surface samples were collected using 47 mm Teflon membrane filters (0.1 µm pore size, Omnipore, Merck Millipore) by slightly wetting the filter, and thus surface, with acetone and subsequently wiping the surface. Surface samples were intended to examine the mass-specific EPFR concentration and relative composition resulting from the combination of the condensed-phase organic film and deposited particulates/dust that are present at the air-surface interface and not sample EPFR present in internal reservoirs (e.g. within building materials). Yet, we acknowledge that these deep layers may be relevant for multiphase chemical reactions.

A representative blank sample using the surface sampling technique on cleaned aluminum foil is shown in Figure S2. The use of high purity Teflon filters was necessary for a good background signal during EPR measurements, that is why materials typically used for surface swabs like Kim wipes (e.g. Diamond et al.)[2] were not employed here. We acknowledge that surface roughness, porosity, and solvent choice could influence surface extraction efficiency, so surface samples were calculated as EPFR concentrations for each sample (i.e., spins μg^{-1}), rather than total EPFR loadings, so bias due to any differences in extraction efficiency across surface types would be limited.

All samples were stored in Analyslide Petri Dishes (Pall Corporation) and wrapped in aluminum foil immediately after collection. To determine the collected sample mass, we weighed each filter before and after collection with a high accuracy balance (+/- 0.01 mg). All the reweighed samples were stored in a freezer at -20 °C or -80 °C until analysis. The -20°C freezer was used for intermediate storage of indoor samples before transfer to the lab -80°C freezer. We do not expect a significant effect from these short temperature differences during storage based on previous studies (e.g. Tong et al. 2018)[3], wherein often -20 °C is the standard for storage of EPFR samples before analysis and the proven long lifetimes of EPFR. Before the EPR test, filter samples were conditioned in a desiccator to prevent potential interferences from condensed water. Afterwards, the samples were cut out of their support ring with a scalpel, folded (which does not affect EPFR content), and packed into a 2 mm ID quartz EPR tube for subsequent measurement.

For EPFR measurements, we set up the EPR spectrometer with the following parameters: 100 kHz modulation frequency; 9.84 GHz microwave frequency; 2.149 mW (20 db) microwave power; 30 db receiver gain; 81.92 ms time constant; 15.48 ms conversion time; 3 G modulation amplitude; 10 scans; and 80-300 G sweep width. After obtaining the EPR spectra of EPFR, the quantification of spins was performed with the Xenon software (Bruker) by double integration of baseline corrected spectra.[1]

For exposure of selected samples to NO_2 and O_3, a part of the filter was manually wrapped around the end of a quartz EPR tube (outer diameter 4 mm) and fixed with Teflon "tape" (a sketch of the experimental setup is shown in Figure S3). This tube was inserted into a 1 cm quartz tube and on the other end connected to

¼ inch Teflon tubing. Via this tubing, we flushed the respective gas mixture through the filter into the 1 cm EPR tube. NO_2 concentrations used in dry N_2 gas were between 50 and 350 ppb, O_3 concentrations in synthetic air exposure experiments were between and 60 and 250 ppb. Blank samples did not show any response in EPFR abundance upon exposure of unsampled filters to O_3 or NO_2 (see Figure S6 for NO_2 blank exposure experiment). We acknowledge that the range of O_3 or NO_2 concentrations used in the reaction experiments sometimes exceed typical indoor concentrations (e.g. Table S4), but a similar setup has been used to examine the reactivity and transformations (setup based on prior work)[4] over shorter experimental timescales (e.g. hours), which may occur over longer real-world timescales indoors. We note that this approach is similar to those used with oxidation flow reactors to examine atmospheric aging with higher oxidant concentrations.[5] During fitting of indoor surface samples with different EPFR types (e.g., Figures 2, S5), a third, smaller EPFR signal was observed in some samples, but the analysis focuses on the more typical type 1 and type 2 EPFR, which exhibit clear response to the O_3 and NO_2 exposure.

An unpaired, one-tailed t-test, assuming heteroscedasticity, between inhabited and uninhabited indoor PM sample sets was used to compare the sample sets with a result of $p < 0.05$, though the associated interpretation in the text is kept limited due to the relatively small sample size and observed variance in each sample set (Figure S4b). For comparison, we note that the exclusion of the last 2 higher concentration inhabited samples (Nov. 18-25, 25-27, Figure 1a) in the t-test, results in a p-value of 0.09.

The prevalence of dust and indoor surfaces used to calculate the EPFR budgets presented in Figure 3b-c were estimated based on the EPFR abundances observed in this study and characteristics of a typical residential space. However, the dust and surface loadings are sensitive to home characteristics, furnishings, and occupant habits so the quantitative breakdown presented is intended to be illustrative with expected variations across the housing stock. While the relative contributions of airborne PM, dust, and surface films are not dependent on the exact home size, a range of volumes (40-400 m^3) were considered (with surface areas 120-1200 m^2). Dust accumulation rates from Thatcher and Layton (1995)[6] were used, which represent dust loadings on certain flooring after one week without vacuuming. The value of 6 ug cm^{-2} for an untracked area of linoleum was scaled up to 10 ug cm^{-2} to account for contributions from various areas of the residence, including at the entryway, while 60 ug cm^{-2} was used for an untracked area of carpet. The average in-home concentration of dust (2 g m^{-3}) was estimated from the average of these two flooring types, to simulate a residence containing both carpet and linoleum/hardwood. For the purposes of this manuscript, a typical surface area to volume ratio of 3 m^{-1} was used, and surface films have been found to approach thicknesses of approximately 15 nm under laboratory conditions and 25 nm in real-world measurements.[7, 8] Since these surface films were assumed to be organic in nature, a density of 1.2 g cm^{-3} for the organic phase was applied based on the range in prior work[8] (0.8-1.7 g cm^{-3}), which arrived at the total surface film concentration within an indoor space (0.36 g m^{-3}). We note that some dust was incorporated into the surface film samples collected here (esp. horizontal surfaces), and as a result the mass-specific EPFR concentration used here (spins μg^{-1}) may be a lower limit of the EPFR content of the condensed organic film (see main text discussion). Gas-phase EPFR were not evaluated in this study but are assumed to be negligible based on the current state of knowledge, and any unforeseen contributions could be expected to be minor in the total indoor EPFR budget, similar to airborne indoor PM (Figure 3b).

Occurrence of other gas-phase species are based on typical literature values for indoor gas-phase oxidants (Table S4). For ozone, the range indicated in Figure 3c is based on the indoor-outdoor ratio reported by the literature[9] (i.e., 0.1 - 0.8), taking the average daily mean value from the observations as a basis. As NO_2 concentrations vary over much smaller spatial scales, the lower threshold in Figure 3c is given by the lowest reported indoor concentration reported in Table S4 (4 ppb) and the upper threshold is given by the highest daily mean value measured outdoors. Particle-phase concentrations of NO_2 and O_3 were estimated via Henry's law using constants reported in the literature,[10] and are intended to examine condensed-phase chemistry, not human exposure to dissolved O_3 or NO_2.

Supplementary Figures and Tables

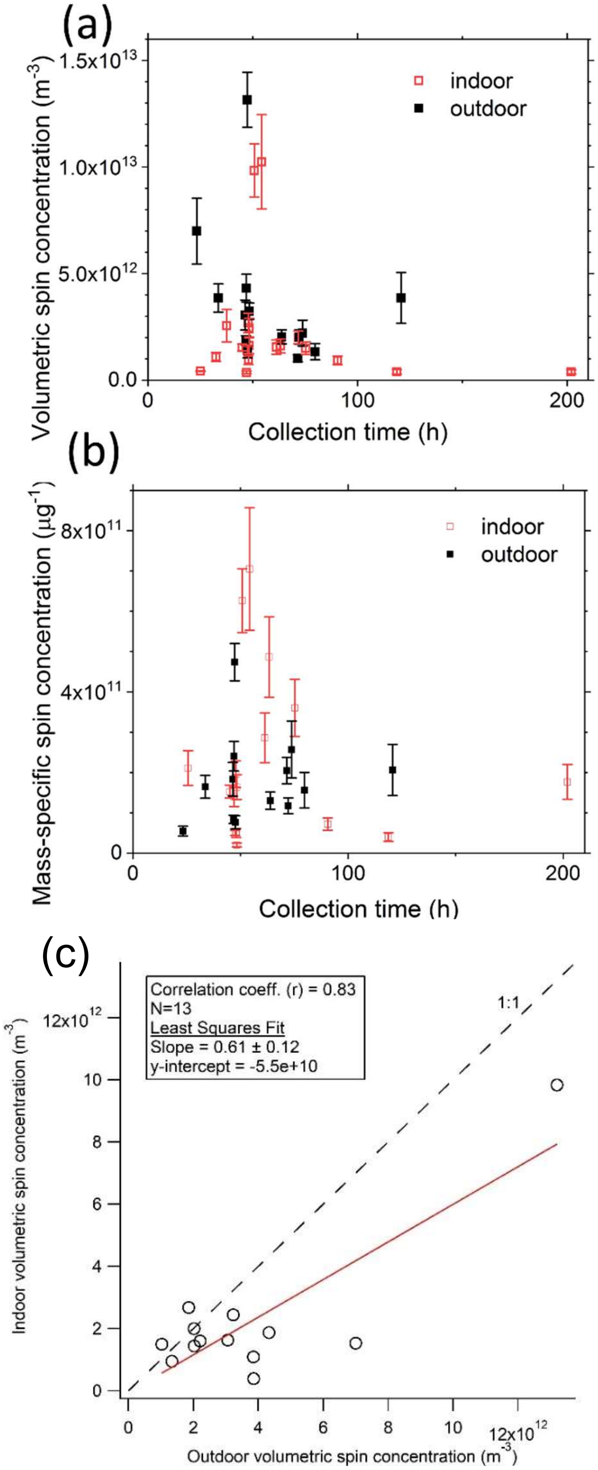

Figure S1: EPFR concentrations in particulate matter (PM) compared to collection time of the respective sample shown as (a) Volumetric spin concentration per volume of sampled air (spins m^{-3}) and (b) Mass-specific EPFR spin concentration per mass of collected particulate matter (spins µg^{-1}). Uncertainties are shown as standard deviations based on repeated analysis of the same sample spectrum. (c) Comparison of indoor vs. outdoor volumetric EPFR concentrations with a least squares regression and a 1:1 line.

Table S1: Sampling details of indoor PM samples, including the total sampled air volume, PM mass, and EPFR abundance.

Sample ID	Collection date (mm/dd/yy)	Sampling details & notes	Sampled air volume (m^3)	PM mass (mg)	EPFR spin abundance (spins)
#23	09/27/19 - 09/28/19	Several cooking events	24.08	not available	1.03E+13
#26	09/28/19 - 10/06/19	Uninhabited except for cleaning visit	193.92	0.43	7.66E+13
#27	10/06/19 – 10/10/19	Inhabited	86.88	1.11	8.03E+13
#28	10/10/19 – 10/12/19	Inhabited	45.12	0.12	1.63E+13
#29	10/12/19 – 10/14/19	Increased ventilation, limited cooking	37.58	0.44	9.22E+13
#30	10/14/19 – 10/16/19	Cooking and cleaning events	45.92	0.63	1.23E+14
#19	10/16/19 – 10/17/19	Cooking events	31.20	not available	3.41E+13
#33	10/17/19 – 10/20/19	Uninhabited with lots of outdoor rain	72.24	0.30	1.08E+14
#32	10/21/19 – 10/23/19	Cleaning and cooking events (incl. oven usage)	45.60	1.31	6.57E+13
#34	10/23/19 – 10/25/19	Some cooking, incl. pan-fried chicken	46.32	0.69	1.13E+14
#35	10/25/19 – 10/28/19	Less cooking, weekend	68.88	not available	1.38E+14
#36	10/28/19 – 10/30/19	Some cooking	46.08	0.88	4.37E+13
#40	10/30/19 – 11/01/19	Cooking events	43.20	0.43	6.61E+13
#41	11/01/19 – 11/03/19	Uninhabited	60.72	0.20	9.73E+13
#43	11/08/19 – 11/11/19	Water leak, minor home repair/construction, higher humidity	58.80	0.32	9.16E+13
#44	11/11/19 – 11/13/19	Smoke from burnt food in oven occurred	46.32	3.76	7.56E+13
#50	11/13/19 – 11/18/19	Partially uninhabited	114.00	1.12	4.47E+13
#52	11/18/19 – 11/25/19	Active mold growth in part of apartment	52.08	0.76	5.34E+14
#53	11/25/19 – 11/27/19	Active mold growth in part of apartment	48.72	0.77	4.79E+14

Note: the first sample was left at ambient temperature for 1 week, but all other samples were immediately put into cold storage as described in the text.

Table S2: Sampling details of outdoor PM samples, including the total sampled air volume, PM mass, and total EPFR spin abundance.

Sample ID	Collection date (mm/dd/yy)	Sampled air volume (m^3)	PM mass (mg)	EPFR spin abundance (spins)
MZ-01	10/12/19 – 10/14/19	47.86	0.86	2.07E+14
MZ-02	10/14/19 – 10/16/19	47.69	1.06	8.87E+13
MZ-03	10/16/19 – 10/17/19	34.25	0.80	1.32E+14
MZ-04	10/17/19 – 10/20/19	72.93	0.37	7.51E+13
MZ-05	10/20/19 – 10/23/19	65.10	1.02	1.32E+14
MZ-37	10/23/19 – 10/25/19	49.30	not available	1.59E+14
MZ-38	10/25/19 – 10/28/19	73.61	1.27	1.49E+14
MZ-39	10/28/19 – 10/30/19	48.53	0.85	6.49E+13
MZ-45	10/30/19 – 11/01/19	23.72	3.03	1.66E+14
MZ-49	11/01/19 – 11/04/19	75.23	0.65	1.66E+14
MZ-46	11/04/19 – 11/07/19	81.35	0.70	1.09E+14
MZ-48	11/11/19 – 11/13/19	47.35	0.79	1.45E+14
MZ-51	11/13/19 – 11/18/19	123.17	2.30	4.75E+14
MZ-58	11/25/19 – 11/27/19	48.28	1.34	6.35E+14

Table S3: Sampling details and results of the collected surface samples and house dust within the apartment investigated in this study.

Sample ID	Collection place	Sampled mass (mg)	Total EPFR Type-1 spin number (spins)	Total EPFR Type-2 spin number (spins)
Surface-01	Kitchen cabinet above oven (horizontal)	21.54	1.66E+14	2.26E+14
Surface-02	Above main room cabinet (horizontal)	0.76	2.94E+12	4.03E+12
Surface-03	Top of bathroom cabinet (horizontal)	3.39	1.82E+13	3.14E+13
Surface-04	Window #1 main room (vertical)	1.01	4.91E+13	9.24E+13
Surface-05	Wall in main bathroom (tile)	1.84	2.15E+08	4.51E+12
Surface-06	Wall in 2nd bathroom (tile outside shower)	0.69	6.36E+08	8.82E+11
Surface-07	Window #2 main room (vertical)	0.90	1.23E+14	1.91E+14
Surface-08	Floor corner main room (horizontal)	8.83	2.92E+14	4.70E+14
Surface-09	Floor corner entry way (horizontal)	15.07	2.06E+14	5.81E+14
Surface-10	Kitchen cabinet above oven (horizontal), adjacent to same area as sample Surface-01	2.57	9.92E+12	1.67E+13
House dust-1	Under couch	3.05	5.91E+13	-
House dust-2	Under couch	1.56	3.49E+13	-

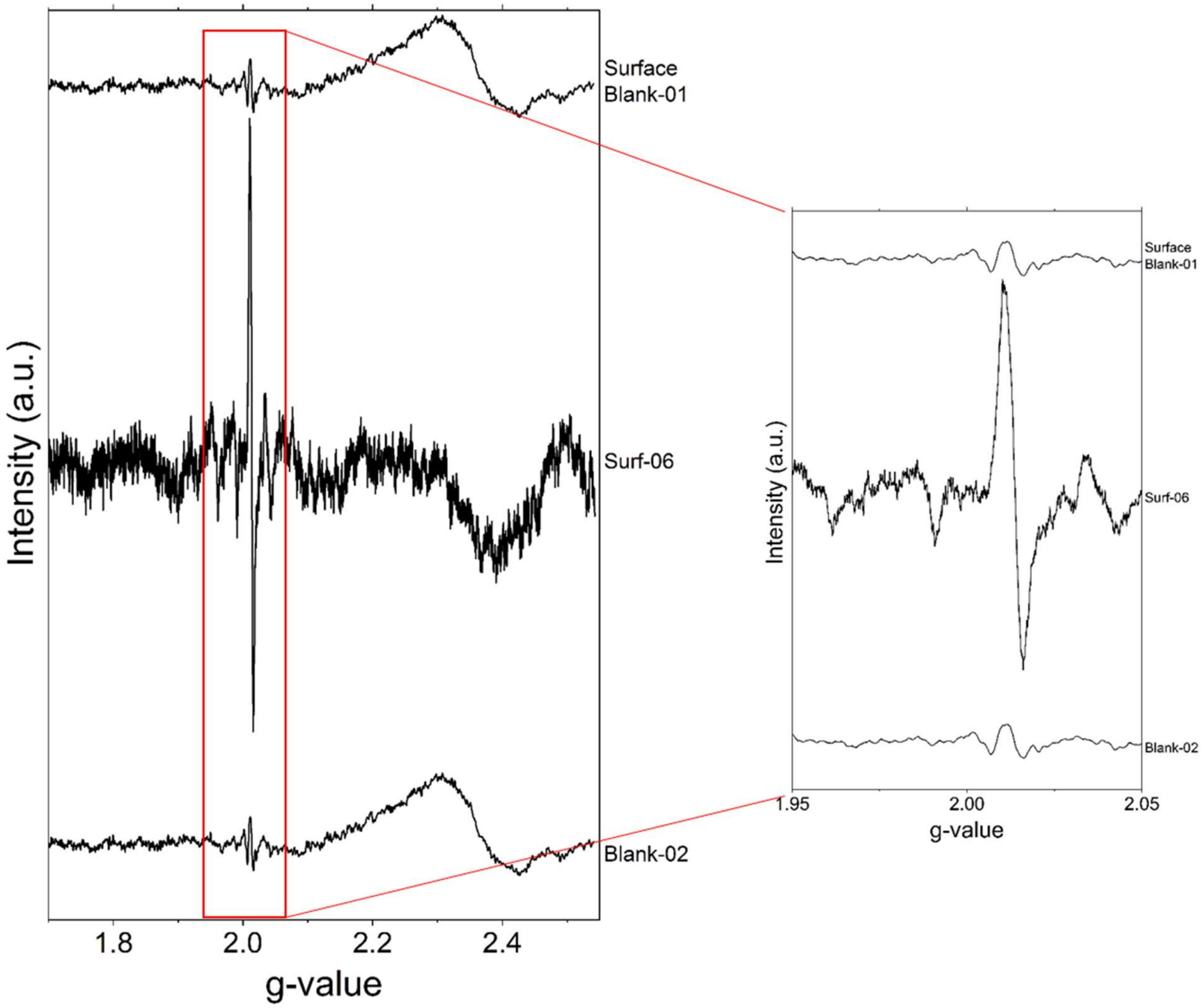

Figure S2: Two surface blank EPR spectra in comparison to a representative surface sample. The panel on the left side shows EPR spectra recorded over a wide magnetic field range, on the right side only the g-value range displayed in Figure S5 is shown.

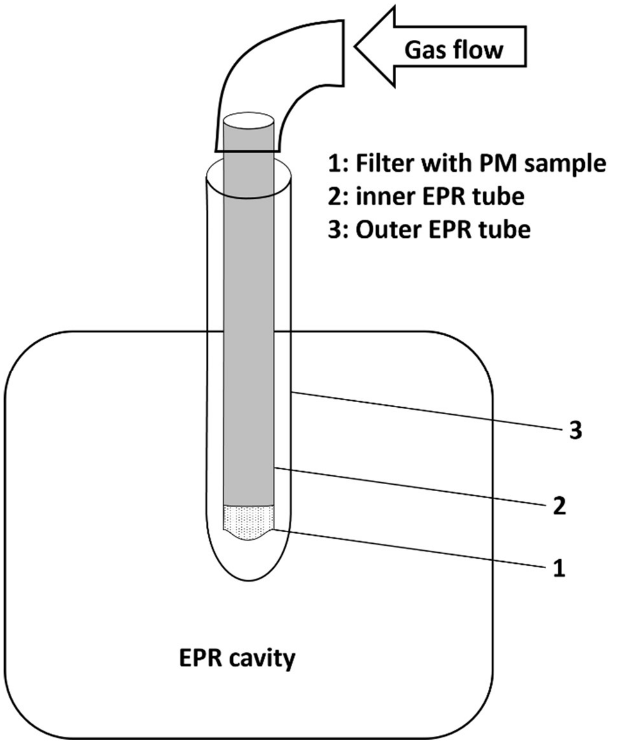

Figure S3: Schematic sketch of the experimental setup used for exposure of samples to reactive gas mixtures containing NO_2 or O_3, where flow comes down the central Teflon tube, exits into the outer EPR tube when the filter sample is positioned in the EPR sensing region, and then exits back out the top.

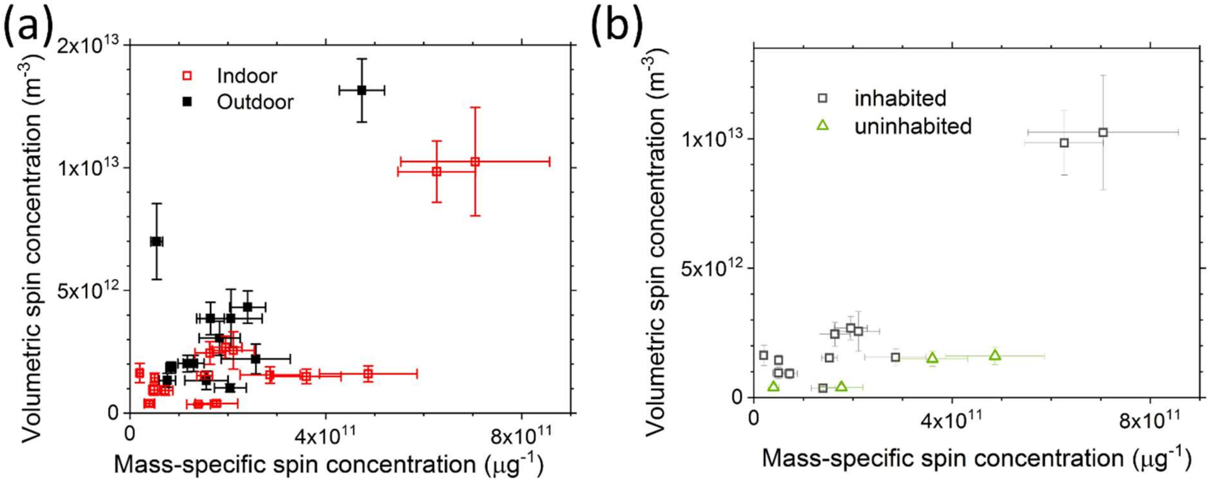

Figure S4: Scatterplots of volumetric and mass-specific EPFR spin concentrations in PM. (a) EPFR concentrations for indoor (empty red squares) and outdoor samples (solid black squares). (b) EPFR concentrations in indoor air differentiated by inhabited (grey squares) and uninhabited periods (light green triangles). Uncertainties are same as those in Figure S1.

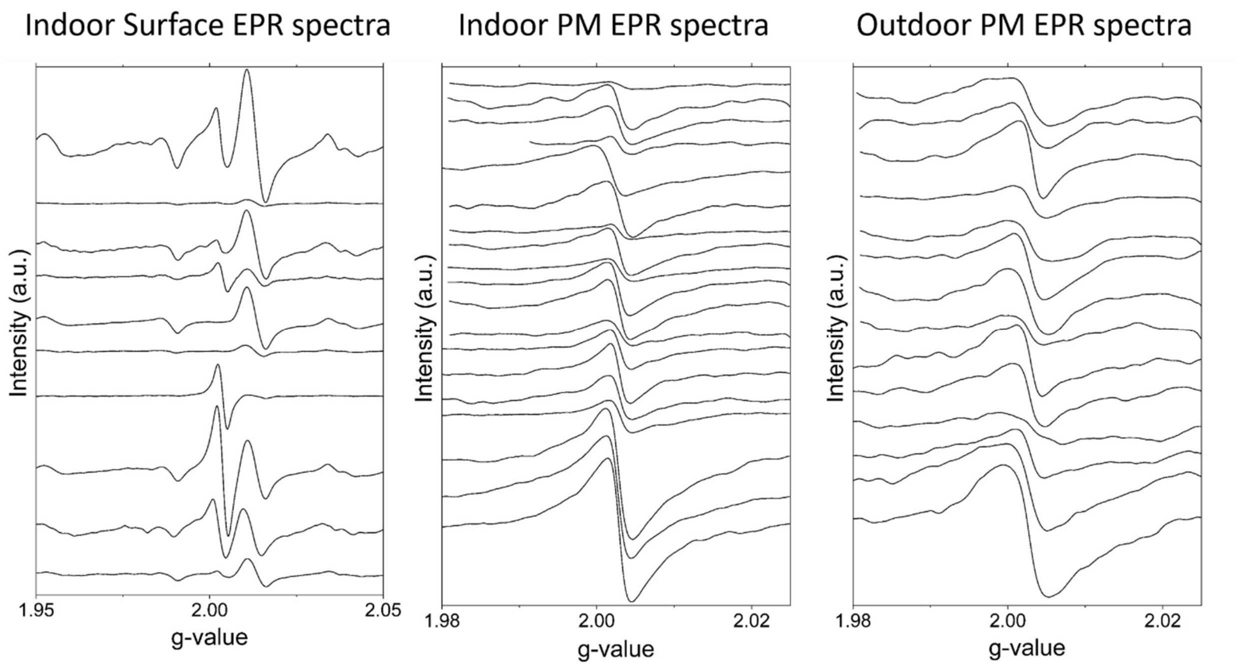

Figure S5: Baseline corrected EPR spectra of all samples collected. The panel on the left side shows indoor surface spectra (sample descriptions can be found in Tables S1-3 along with the breakdown of Type 1 and Type 2 EPFR in Table S3 for surfaces and dust). The panel in the center shows indoor PM spectra and the panel on the right side shows outdoor PM. The y-axis dimensions are conserved within the respective panels, and samples are listed in numerical order from top to bottom, corresponding to the order in Tables S1-3 and the spectra shown here are not normalized for mass or volume collected.

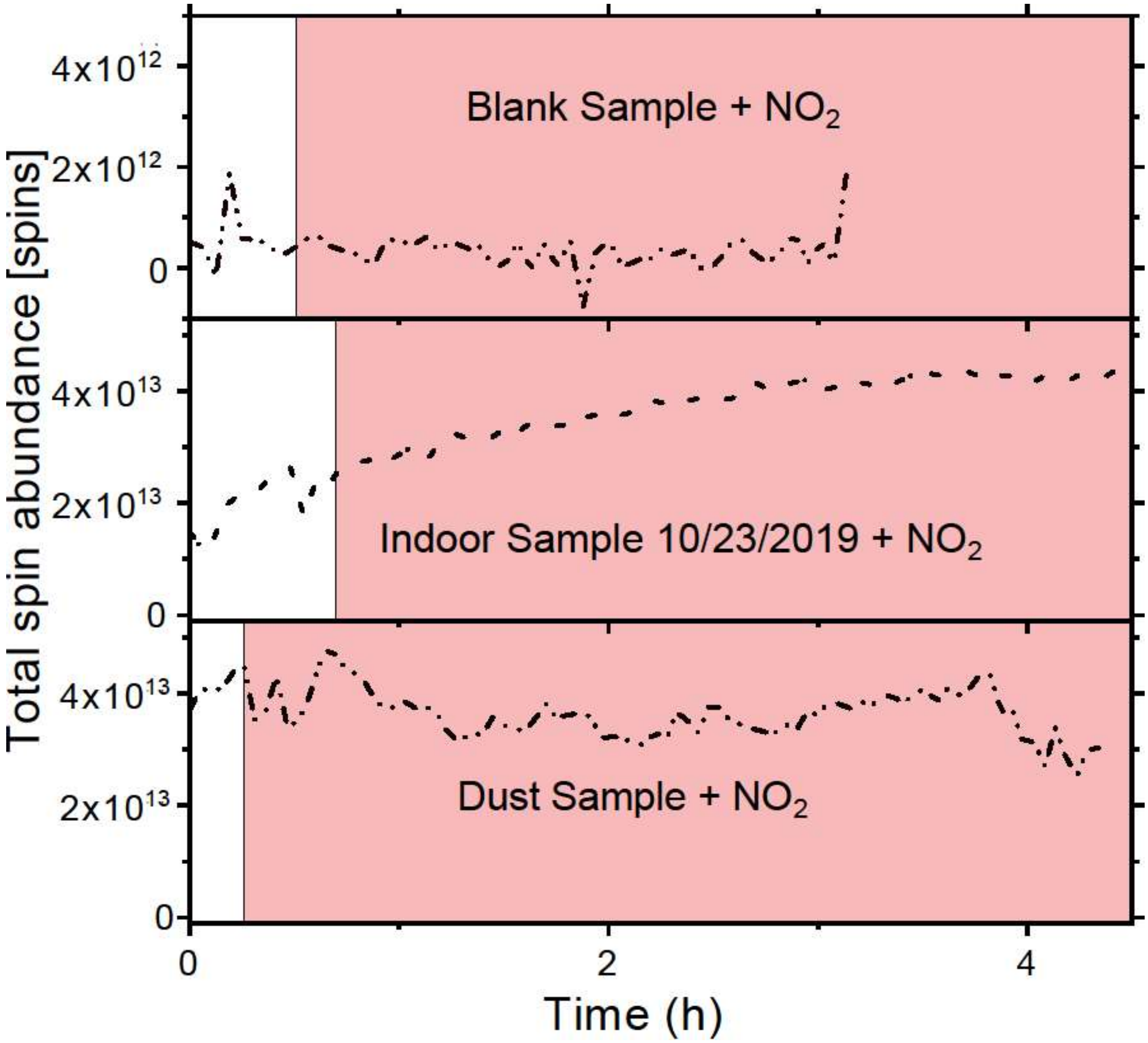

Figure S6: Total spin abundance of EPFR Type-1 upon exposure of the respective (top: blank; middle: indoor PM, bottom: dust) samples to NO_2. The figure shows the integrated spin abundance, starting from the beginning of the exposure experiment when samples were flushed with dry nitrogen gas for equilibration (unshaded). The red shaded area illustrates the time when dry nitrogen gas with 50-350 ppb NO_2 was added. The middle plot corresponds to the indoor PM sample from 10/23/2019. The integrated signal plotted for the blank filter sample is detector noise, which is why the indicated concentration is so small compared to the others.

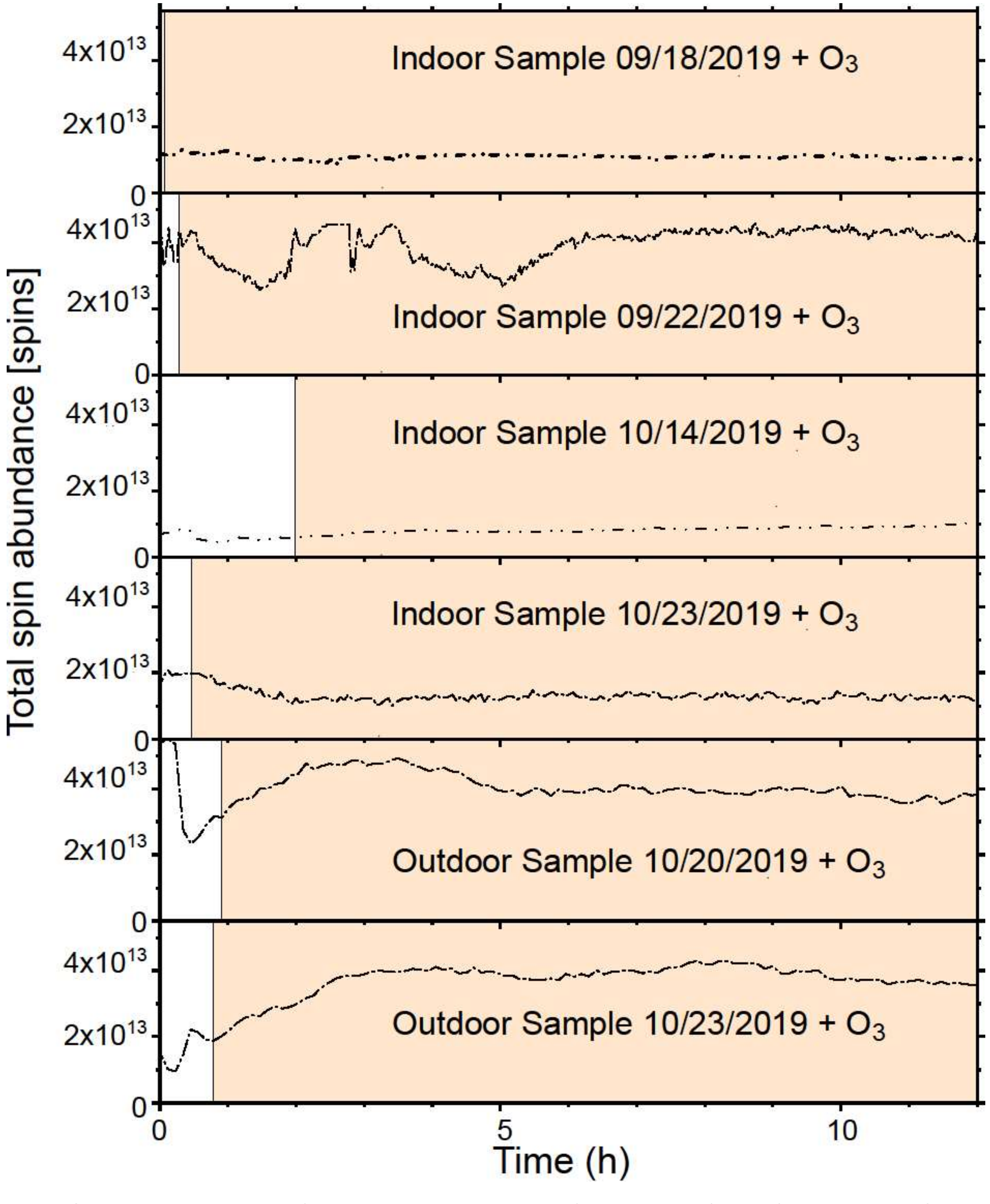

Figure S7: Total spin abundance of EPFR Type-1 upon exposure of the respective (labelled) PM samples to O_3. The figure shows the integrated spin abundance from the start of the exposure experiment, when samples were flushed with dry nitrogen gas for equilibration (unshaded). The yellow shaded area illustrates the time when dry nitrogen gas with 60-250 ppb O_3 began flowing through the online EPR setup. Surface sample exposure experiments for ozone (and NO_2) are shown in the main text (Figure 2).

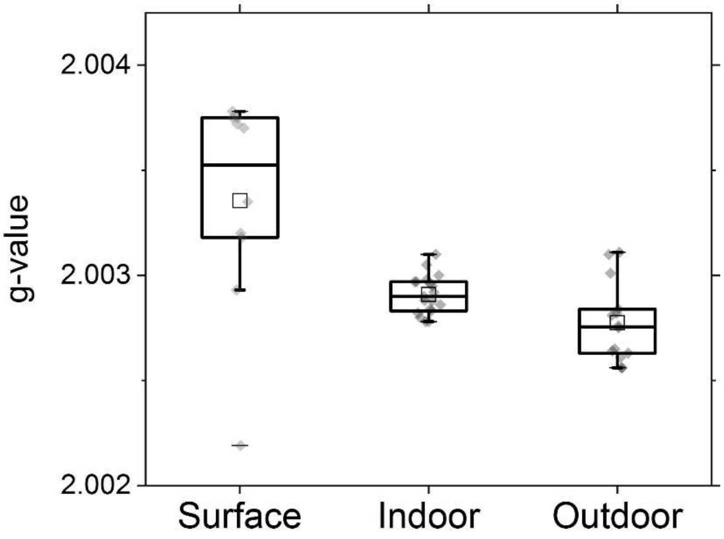

Figure S8: Box plot of average g-values of Type 1 EPFR signal from indoor surfaces, indoor PM, and outdoor PM, taking into account all samples from each respective group collected during this study. Shown with individual data points from each sample.

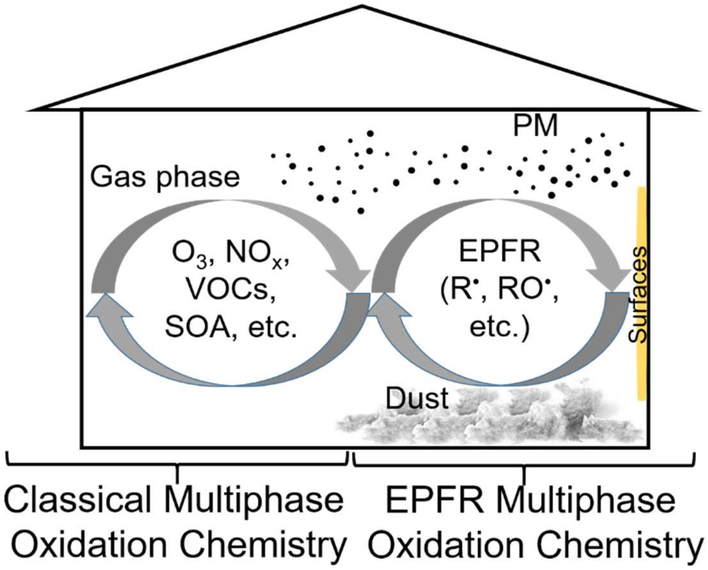

Figure S9: A proposed, simplified schematic of classical and EPFR-related oxidation chemistry.

Table S4: Literature values on ozone (O_3) and nitrogen dioxide (NO_2) concentrations in indoor environments.

O_3 (ppb)			**NO_2 (ppb)**		
Reference	Mean	Range	Reference	Mean	Range
(Lee et al., 2002)[11]	14.9	0.6 - 67.8	(Lee et al., 2002)[11]	28.0	4.3 - 52.0
(Zhang and Lioy, 1994)[12]	28.0	1.0-181.0	(Zhou et al., 2018)[13]	3.7	20.0 (other studies: 4.8 - 46.5)
(Zhang et al., 1994)[14]		30.0-60.0	(Weschler, 2000)[15]	30.0	
(Hwang and Park, 2020)[16]	11.4		(Hwang and Park, 2020)[16]	13.9	
(Zhou et al., 2019)[17]	0.6 (residence) 21.5 (lab) 22.5 (office)		(Zhou et al., 2019)[17]	8.4 (residence) 9.1 (lab) 11.3 (office)	
(Abbatt and Wang, 2020)[9]	< 5.0	0.1 - 0.8 of outdoor air			

References

1. A. M. Arangio, H. Tong, J. Socorro, U. Pöschl and M. Shiraiwa, Quantification of environmentally persistent free radicals and reactive oxygen species in atmospheric aerosol particles, *Atmospheric Chemistry and Physics*, 2016, **16**, 13105-13119.
2. M. L. Diamond, S. E. Gingrich, K. Fertuck, B. E. McCarry, G. A. Stern, B. Billeck, B. Grift, D. Brooker and T. D. Yager, Evidence for organic film on an impervious urban surface: characterization and potential teratogenic effects, *Environmental Science & Technology*, 2000, **34**, 2900-2908.
3. H. Tong, P. S. Lakey, A. M. Arangio, J. Socorro, F. Shen, K. Lucas, W. H. Brune, U. Pöschl and M. Shiraiwa, Reactive oxygen species formed by secondary organic aerosols in water and surrogate lung fluid, *Environmental science & technology*, 2018, **52**, 11642-11651.
4. F. Liu, P. S. Lakey, T. Berkemeier, H. Tong, A. T. Kunert, H. Meusel, Y. Cheng, H. Su, J. Fröhlich-Nowoisky and S. Lai, Atmospheric protein chemistry influenced by anthropogenic air pollutants: nitration and oligomerization upon exposure to ozone and nitrogen dioxide, *Faraday discussions*, 2017, **200**, 413-427.
5. B. B. Palm, P. Campuzano-Jost, D. A. Day, A. M. Ortega, J. L. Fry, S. S. Brown, K. J. Zarzana, W. Dube, N. L. Wagner and D. C. Draper, Secondary organic aerosol formation from in situ OH, O 3, and NO 3 oxidation of ambient forest air in an oxidation flow reactor, *Atmospheric Chemistry and Physics*, 2017, **17**, 5331-5354.
6. T. L. Thatcher and D. W. Layton, Deposition, resuspension, and penetration of particles within a residence, *Atmospheric environment*, 1995, **29**, 1487-1497.
7. C. M. Eichler, J. Cao, G. Isaacman‐VanWertz and J. C. Little, Modeling the formation and growth of organic films on indoor surfaces, *Indoor Air*, 2019, **29**, 17-29.
8. C. J. Weschler and W. W. Nazaroff, Growth of organic films on indoor surfaces, *Indoor Air*, 2017, **27**, 1101-1112.
9. J. P. Abbatt and C. Wang, The atmospheric chemistry of indoor environments, *Environmental Science: Processes & Impacts*, 2020, **22**, 25-48.
10. R. Sander, Compilation of Henry's law constants (version 4.0) for water as solvent, *Atmos Chem Phys*, 2015.
11. K. Lee, J. Xue, A. S. Geyh, H. Ozkaynak, B. P. Leaderer, C. J. Weschler and J. D. Spengler, Nitrous acid, nitrogen dioxide, and ozone concentrations in residential environments, *Environmental health perspectives*, 2002, **110**, 145-150.
12. J. Zhang, P. J. Lioy and Q. He, Characteristics of aldehydes: concentrations, sources, and exposures for indoor and outdoor residential microenvironments, *Environmental science & technology*, 1994, **28**, 146-152.
13. S. Zhou, C. J. Young, T. C. VandenBoer, S. F. Kowal and T. F. Kahan, Time-resolved measurements of nitric oxide, nitrogen dioxide, and nitrous acid in an occupied New York home, *Environmental science & technology*, 2018, **52**, 8355-8364.
14. J. Zhang and P. J. Lioy, Ozone in residential air: concentrations, I/O ratios, indoor chemistry, and exposures, *Indoor Air*, 1994, **4**, 95-105.
15. C. J. Weschler, Ozone in indoor environments: concentration and chemistry, *Indoor air*, 2000, **10**, 269-288.
16. S. H. Hwang and W. M. Park, Indoor air concentrations of carbon dioxide (CO 2), nitrogen dioxide (NO 2), and ozone (O 3) in multiple healthcare facilities, *Environmental geochemistry and health*, 2020, **42**, 1487-1496.
17. S. Zhou, C. J. Young, T. C. VandenBoer and T. F. Kahan, Role of location, season, occupant activity, and chemistry in indoor ozone and nitrogen oxide mixing ratios, *Environmental Science: Processes & Impacts*, 2019, **21**, 1374-1383.